Title

DETERMINATION OF TRANSVERSE SHIELDING FOR PROTON ACCELERATORS USING THE MOYER MODEL

Authors

Stevenson, G.R.
Kuei-Lin, L.
Thomas, R.H.

Publication Date

1981-02-01

Lawrence Berkeley Laboratory
UNIVERSITY OF CALIFORNIA

Engineering & Technical Services Division

Submitted to Health Physics

DETERMINATION OF TRANSVERSE SHIELDING FOR PROTON ACCELERATORS USING THE MOYER MODEL

Graham R. Stevenson, Liu Kuei-Lin, and Ralph H. Thomas

February 1981

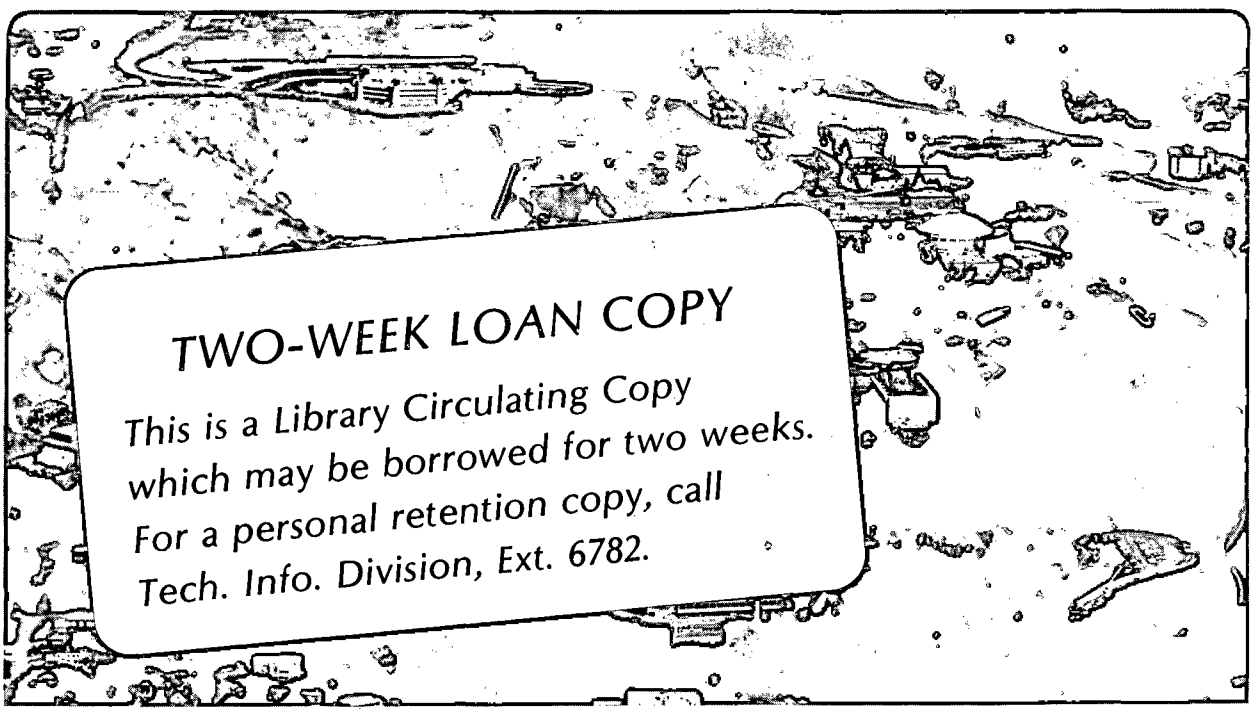

Prepared for the U.S. Department of Energy under Contract W-7405-ENG-48

DISCLAIMER

To be submitted
to Health Physics

LBL-11337
CERN-HS-RP/049/PP
BPS-HS 8011

DETERMINATION OF TRANSVERSE SHIELDING FOR PROTON ACCELERATORS USING THE MOYER MODEL

Graham R. Stevenson
CERN, Geneva, Switzerland

Liu Kuei-Lin
Beijing Proton Synchrotron
Institute of High Energy Physics
Beijing, China

Ralph H. Thomas
Lawrence Berkeley Laboratory
University of California
Berkeley, California 94720
USA

This work was supported by the European Centre for Nuclear Research, Geneva; by the Institute of High-Energy Physics, Academia Sinica, Beijing; and by the U.S. Department of Energy under Contract No. W-7405-ENG-48 with the University of California.

CONTENTS

LIST OF FIGURES

LIST OF TABLES

DETERMINATION OF TRANSVERSE SHIELDING FOR PROTON ACCELERATORS USING THE MOYER MODEL

Graham R. Stevenson
CERN, Geneva, Switzerland

Liu Kuei-Lin
Beijing Proton Synchrotron
Institute of High Energy Physics
Beijing, China

Ralph H. Thomas
Lawrence Berkeley Laboratory
University of California
Berkeley, California
USA

ABSTRACT

The historical development of the Moyer Model - an empirical method used in the design of high energy proton accelerator shielding - is described. With the improvements in the understanding of high-energy radiation phenomena which have occurred during the past twenty years it is now possible to lay a more satisfactory theoretical basis for this model. Several measurements at various high energy proton accelerators now make it possible to improve the parameters used in the model and consequently to increase its accuracy. An example of the use of the model to calculate transverse shielding for an extended uniform line source is given and comparison made with calculations by O'Brien.

1. Introduction

The design and construction of the first proton accelerators in the GeV energy region during the fifties and early sixties demanded an increased understanding of high-energy particle accelerators radiation environments (Pa 73). Control of the intensity of the radiation field around these accelerators - to permit safe and efficient operations - by the design of radiation shielding became an urgent task following experience obtained with the early operation of the Cosmotron and Bevatron (So 57).

At that time there was no firm theoretical basis for designing accelerator shielding and, in consequence, semi-empirical methods were developed. Perhaps the most useful and widely known of these models is the "Moyer Model" (Mo 61, Mo 62).

This paper describes the historical development of the model, discusses it in the light of our understanding of high-energy radiation transport phenomena, summarizes determinations of the Moyer Model parameters at several high-energy proton accelerators and, finally, discusses the limitations of the Model and its value in accelerator shield design.

2. The Moyer Model

In 1961 Moyer described a semi-empirical method for determining the shielding required for the Bevatron - the 6 GeV proton synchrotron of the then University of California Radiation Laboratory (Mo 61, Mo 62) - whose intensity was to be substantially increased (We 63). This model - later called the "Moyer Model" - "Provides a formalism to evaluate the high energy neutron fluxes and associated biological dose-rates outside the

main shield of the accelerator, in places where the nucleon-meson cascade is well-developed and essentially in equilibrium" (Ro 72).

Many descriptions of the Moyer Model have been published in the literature (Pa 73). In these earlier descriptions the authors have concentrated on a discussion of the neutron component of the radiation field. This was principally because neutrons make the dominant contribution to dose equivalent outside well-shielded proton accelerators (Pe 66). Although high-energy neutrons are not the only particles that play an important role in propagating the hadronic cascade in matter it was sufficiently accurate at that time to treat all hadronic cascade propagators as "neutron like."

The fact that those neutrons which largely contribute to the dose equivalent ($E \leqslant 50$ MeV) are not those that propagate the hadronic cascade ($E > 150$ MeV) has led to some confusion in understanding the early literature.

As we shall show later the formalization used in the early papers describing the Moyer Model is essentially unchanged by our increased understanding of high-energy radiation transport and so will be repeated here. The treatment given is that by Rindi and Thomas (Ri 73).

Consider an effective point source produced by protons interacting in a thin target (Fig. 1). Assuming that neutrons are the only secondary particles to be considered the radiation level on the outside of a shield may be written by as

$$H = \frac{1}{r^2} \int F(E)\ B(E,\theta)\ \exp\left[-d(\theta)/\lambda(E)\right] \frac{d^2n(E,\theta)}{dE\ d\Omega} \cdot dE \qquad (1)$$

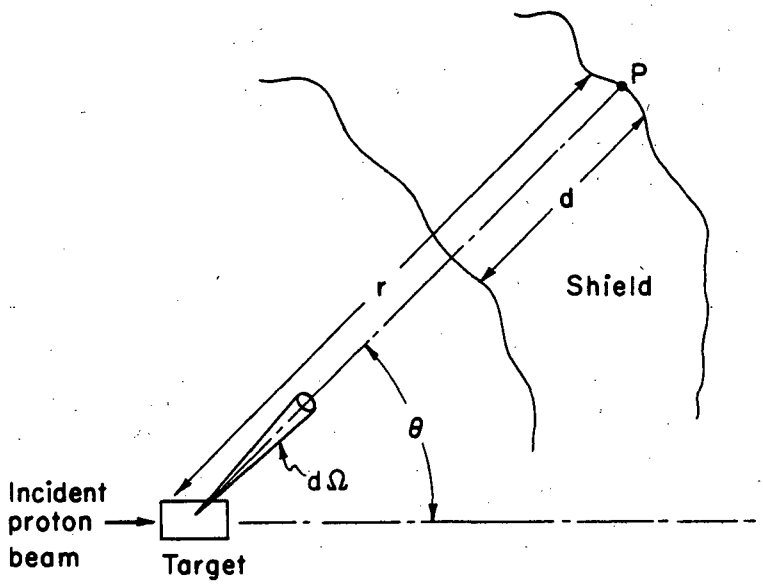

Fig. 1. Schematic diagram of typical shielding geometry.

where r is the distance from the source, E is the neutron energy, F is a factor which converts fluence to dose equivalent, d is the shield thickness, λ is the effective removal mean-free path, B is a buildup factor, and $d^2n/dE\ d\Omega$ is the yield of neutrons per unit solid angle at angle θ, per unit energy interval at E.

De Staebler (De 62) wrote Eq. (1) as:

$$H = r^{-2} \sum_i B_i F_i \exp(-d/\lambda_i) \cdot (dn/d\Omega)_i \qquad (2)$$

where the subscript i denotes a range of neutron energies for which B, F, and λ are fairly constant and the definition of $(dn/d\Omega)$ is obvious.

Neutron attenuation lengths above 150 MeV are roughly independent of energy, but diminish rapidly with energy below about 100 MeV. Consequently the greater yields of low-energy, as compared to high-energy, neutrons at the primary interaction will be more than compensated for by the greater attenuating action of the shield for these neutrons. Moyer (Mo 61, Mo 62) made an extremely important contribution when he recognized that Eq. (2) may be approximated by a single-energy group because the nature of the radiation field outside the shield of a high-energy proton accelerator will be determined by neutrons with energy greater than about 150 MeV. In fact, because high-energy pions and protons in the hadronic cascade have very similar cross sections to neutrons we may talk of "cascade propagators" rather than just high-energy neutrons. Deep in the shield, these high-energy (E > 150 MeV) hadrons regenerate the cascade but are present in relatively small numbers. At a shield interface the radiation field observed consists of these "propagators," born close to the primary radiation source,

accompanied by many particles of much lower energy, mainly neutrons, born near the interface.

The total neutron flux density (and consequently the dose-equivalent rate) will be proportional to the high-energy hadron flux density. Because the low-energy components are produced by interaction of the high-energy propagators, their intensity decreases through the shield in an exponential manner with effectively the same attenuation length for all directions through the shield.

The essence of the Moyer Model, therefore, is that the dose equivalent at any point outside the accelerator shield is largely governed by the simple "line-of-sight" propagation of the cascade generating particles produced at the first interaction (target) and a multiplication factor may be used to account for particle build up. The cascade-generating particles have an attenuation length which is independent of energy.

Several experimental verifications of Moyer's basic assumptions have been reported in the literature. In a series of measurements in concrete irradiated by protons with energy between 2.2 and 6.2 GeV, Smith et al. (Sm 65a) demonstrated the essential independence of radiation attenuation length with radiation detector and also with angle to the incident proton beam direction, and with a threshold of the neutron detector used. Smith (Sm 65b) has described the excellent agreement between measured radiation levels around the Bevatron and those predicted by Moyer. In that series of measurements the development of radiation field equilibrium was also demonstrated. Gilbert et al. (Gi 68, Gi 69) showed that the Moyer Model was able to account for neutron flux densities in the earth shielding of

the CERN 25 GeV proton synchrotron with good accuracy. Over a range of 10^5 in flux density and up to a distance of 40 meters from an internal target in the accelerator, which was the principal source of radiation during the measurements, typical results gave an accuracy in neutron flux density estimation of 20% or better (Gi 68).

In practical shield configurations, the combined effect of angular distribution and attenuation means that the transverse thickness of a shield is dominated by the hadrons emitted at angles between about 60^o and 120^o. $B(E,\theta)$ then loses its angular dependence since the spectrum can be assumed to be invariant over this limited range of angles. Also, since now one is dealing with the global fluence of particles above 150 MeV, B(E) can be replaced by m(Ep) which is constant for a given target material and primary proton energy, E_p.

One can also write

$$\int_{E > 150 \text{ MeV}} \frac{d^2n(E,\theta)}{dE\, d\Omega}\, dE = g(\theta) \qquad (4)$$

where $g(\theta)$ is the angular distribution function for hadrons with energy greater than 150 MeV.

Thus

$$\phi\ (E > 150 \text{ MeV}) = g(\theta) r^{-2} \exp(-x/\lambda)\ m(E_p) \quad . \qquad (5)$$

For an equilibrium cascade the total dose equivalent is proportional to the fluence of hadrons with energy above 150 MeV.

$$H = k\phi\ (E > 150 \text{ MeV})$$

and over the range of interest $g(\theta)$ can be approximated by an exponential of the form

$$g(\theta) = C \exp(-\beta\theta) \quad . \tag{6}$$

Thus the dose equivalent can be estimated from first principles, as Moyer did, from an equation of the form

$$H = kC\, m(E_p) r^{-2} \exp(-\beta\theta) \exp(-x/\lambda) \quad . \tag{7}$$

It is possible to reduce this equation to a more simple form by combining the many constants in the above expression into one empirically determined constant $H_o(E_p)$:

$$H = H_o(E_p) r^{-2} \exp(-\beta\theta) \exp(-x/\lambda) \quad . \tag{8}$$

$H_o(E_p)$ can be determined from experimental data. Also since the $\theta = 90^o$ case is the one that most often enters into practical consideration, one can further simplify:

$$H = H_1(E_p) r^{-2} \exp\,[-x/\lambda] \tag{9}$$

where H_1 is the apparent dose equivalent at unit distance from the target at 90^o.

H_1 may be related to H_o by substituting $\theta = \pi/2$ into Eq. (8):

$$H = H_o(E_p) r^{-2} \exp(-\beta\pi/2) \exp(-x/\lambda) \tag{10}$$

and comparing with Eq. (9) it follows:

$$H_1(E_p) = H_o(Ep)\ \exp(-\beta\pi/2) \quad . \qquad (11)$$

It will then later be shown that the best value of β determined by measurement is 2.3. Substituting into Eq. (11) we obtain:

$$H_1(E_p) = 2.70 \times 10^{-2}\ H_o(E_p) \quad .$$

3. Moyer Model Parameters

The three Moyer Model parameters, H_o, β and λ must be determined experimentally. The first two, H_o and β may depend upon incident proton energy and primary target material while the third (λ) is, as we have seen, essentially energy independent but will depend upon shield material.

In this section experimental determinations of the Moyer Model Parameters at Argonne National Laboratory, Brookhaven National Laboratory, CERN and the Rutherford Laboratory will be summarized.

(i) 1966 CERN-LRL-RHEL Shielding Experiment (1966).

One of the most extensive high-energy accelerator shielding experiments was carried out on the CERN 25 GeV proton synchrotron (CPS) by a team drawn from CERN, the Lawrence Berkeley Laboratory and the Rutherford Laboratory. This experiment (referred to as the CLR experiment) has been described in great detail and the interested reader who wishes to further his understanding of these measurements is referred to the original paper (Gi 68).

Measurements of neutron flux density were made in several locations in the earth shield surrounding an internal aluminum target bombarded by protons of 13.7 and 25.5 GeV. Measurements were made using activation detectors (primarily the $^{27}Al \rightarrow {}^{24}Na$ and $^{12}C \rightarrow {}^{11}C$ reactions, referred to in what follows as the Al and C reactions). The analysis of this experiment proceeded by expressing the flux density at a point in terms of five factors:

(1) A source distribution term : $\{1 + a_1 \exp(-a_3 z)\}$

(2) An angular distribution term : $a_2 \exp(-a_4 \theta)$

(3) Two attenuation terms, one for the magnet iron and one for the earth shield, : $\exp(-\ell_{Fe}/a_5)$ and $\exp(-\ell_E/a_6)$

(4) An inverse square law term.

The flux density at a point p, ϕ_p, is then given by the Moyer-type expression:

$$p = a_9 \int_{-\infty}^{+\infty} \frac{\{1 + a_1 \exp(-a_3 Z)\}\ a_2 \exp(-a_4 \theta)\ \exp(-\ell_{Fe}/a_5)\ \exp(-\ell_E/a_6)}{(Z-Z_i)^2 + V_i^2}\ dz. \qquad (12)$$

Here we follow the original notation of Gilbert et al. (Gi 68) for the parameters a_1, a_2 ... a_9. Two parameters - a_7 and a_8 - do not appear here. They were used by the authors to express particle buildup. For our purposes $a_7 = a_8 = 0$ and the corresponding buildup factor is therefore unity.

In Eq. (12) ℓ_{Fe} and ℓ_E are the shield thicknesses corresponding to the point (Z_i, V_i) at which the flux density was measured. Equation (12) may be seen to have seven free parameters, $a_1 - a_9$ inclusive. a_9 is a global normalization parameter.* Gilbert et al. (Gi 68) were able to use a least squares fitting analysis to obtain values of these parameters. Initial analysis showed that the exact value of the attenuation length in iron, a_5, did not profoundly influence the quality of the fit to the data. It was therefore fixed at a value of 0.2 m (1500 kg m^{-2}) to simplify further analysis. The number of free parameters in Eq. (4) is therefore reduced to five: a_1, a_3, a_4, a_6 and the product a_2a_9. Of these a_1 and a_3 relate to the beam loss distribution and only a_4, a_6, and the product of a_2a_9 are of interest in determining the Moyer Model parameters.

Gilbert et al. (Gi 68) showed that the attenuation length in earth, a_6, was well constrained and had the value 1170 $\pm$ 20 kg m^{-2}.

The angular distribution parameter, a_4, was not so well constrained - values in the range 2.1 to 2.4 rad^{-1} being obtained. A value of 2.2 was assumed to be the "best" value, independent of the proton energy. The beam loss parameters gave the "best fit" values of a_1 = 220 m and a_3 = 0.15 m^{-1} also independent of E_p.

The values obtained for the normalization constant $a_2 \cdot a_9$ are summarized in Table 1 (taken from Table XC of Gi 68), all values being normalized to a circulating beam current of 1.0×10^{12} pps.

---

*See Gilbert et al. (Gi 68).

appropriate values of H_1 have been calculated from the value of H_o and the fitted value of a_4, (or β). These values are also listed in Table 1.

a_9 is related to the number of lost or interacting protons, i.e., the number of protons lost between z and z + dz = $a_9 \{1 + a_1 \exp(-a_3 z)\} \cdot dz$. The constant a_2 has the same significance as that of H_o in section 2 of this paper, viz. the measured flux density (or dose equivalent rate) per interacting proton. In the experiment of Gilbert et al. (Gi 68) the number of protons lost in the target region (0.54×10^{12} protons s^{-1} in Run II and 0.50×10^{12} protons s^{-1} in Run VII) may be set equal to

$$\int_0^{628m} a_9 a_1 \exp(-a_3 Z)\, dZ \quad .$$

a_9 has the values 3.7×10^8 pps.m^{-1} and 3.4×10^8 pps.m^{-1} for the 13.7 and 25.5 GeV runs respectively. The values of a_2 are then those appearing in Table 1. These have been converted to dose equivalent using the conversions (Gi 68):

$1\ n\ m^{-2} \equiv 9.3 \times 10^{-14}$ Sv for the C detectors.*

$1\ n\ m^{-2} \equiv 2.9 \times 10^{-13}$ Sv for the Al detectors.*

---

*In the original reference the conversion factors are given as:

$3.0\ n\ cm^{-2}\ s^{-1} = 10^{-3}$ rem h^{-1} for the C detectors.

$0.95\ n\ cm^{-2}\ s^{-1} = 10^{-3}$ rem h^{-1} for the Al detectors.

Table 1. Values of the normalizing constants a_4, H_o and H_1.

Energy (GeV)	Run*	Detector	$a_2 a_9$ ($m^{-1}\ s^{-1}$)	a_2 ($m^{-2}\ s^{-1}$)	a_4 (rad^{-1})	$H_o(E_p)$ ($Sv \cdot m^2$)	$H_1(E_p)$ ($Sv \cdot m^2$)
13.7	VII	C	9.16×10^9	2.69×10^1	2.1-2.4	2.5×10^{-12}	7.8×10^{-14}
13.7	VII	Al	3.47×10^9	1.02×10^1		3.1×10^{-12}	9.4×10^{-14}
25.5	II	C	1.29×10^{10}	3.49×10^1		3.3×10^{-12}	1.0×10^{-13}
25.5	II	Al	6.15×10^9	1.66×10^1		5.0×10^{-12}	1.5×10^{-13}

*See Gilbert et al. (Gi 68).

ii) Rutherford Laboratory Measurements

Stevenson et al. have reported measurements with 7.4 GeV protons incident upon a thick tungsten target (Sh 69, St 69). Al and C detectors were again used to measure the flux densities. The normalized flux densities have been multiplied by the square of the detector-target distance in meters and by the attenuation factors in iron and concrete; these values are shown plotted in Fig. 2. This gives the function $g(\theta)$ according to the equation:

$$g(\theta) = H_o \cdot \exp(-\beta \cdot \theta) = H \cdot r^2 \cdot \exp(x_{Fe}/\lambda_{Fe}) \cdot \exp(x_C/\lambda_C) \qquad (13)$$

where Fe and C refer to the parameters for iron and concrete respectively. The value for λ_C was chosen to be 1170 $kg \cdot m^{-2}$ (Gi 68). In their original analysis Stevenson et al. used a value of 1650 $kg \cdot m^{-2}$ for the attenuation length in iron. This value is probably too high. The data of Gilbert et al. (Gi 68) are consistent with a value of 1470 $kg \cdot m^{-2}$ and in Fig. 2 the data shown have been recalculated from the originally published data using this latter value of λ_{Fe}. The parameters H_1 and β determined from these data are given in Table 2.

(iii) Argonne National Laboratory (1966)

Howe et al. (Ho 66) have described measurements of absorbed dose rate in the concrete shielding (ρ = 3800 $kg \cdot m^{-3}$) around a copper target bombarded by 10 GeV protons.

Dose equivalent rates were determined from measurements with tissue equivalent chambers and an LET spectrometer. Film badges were also used to obtain a relative measure proportional to dose equivalent. (The film badge calibration did not permit absolute dose estimates to be made).

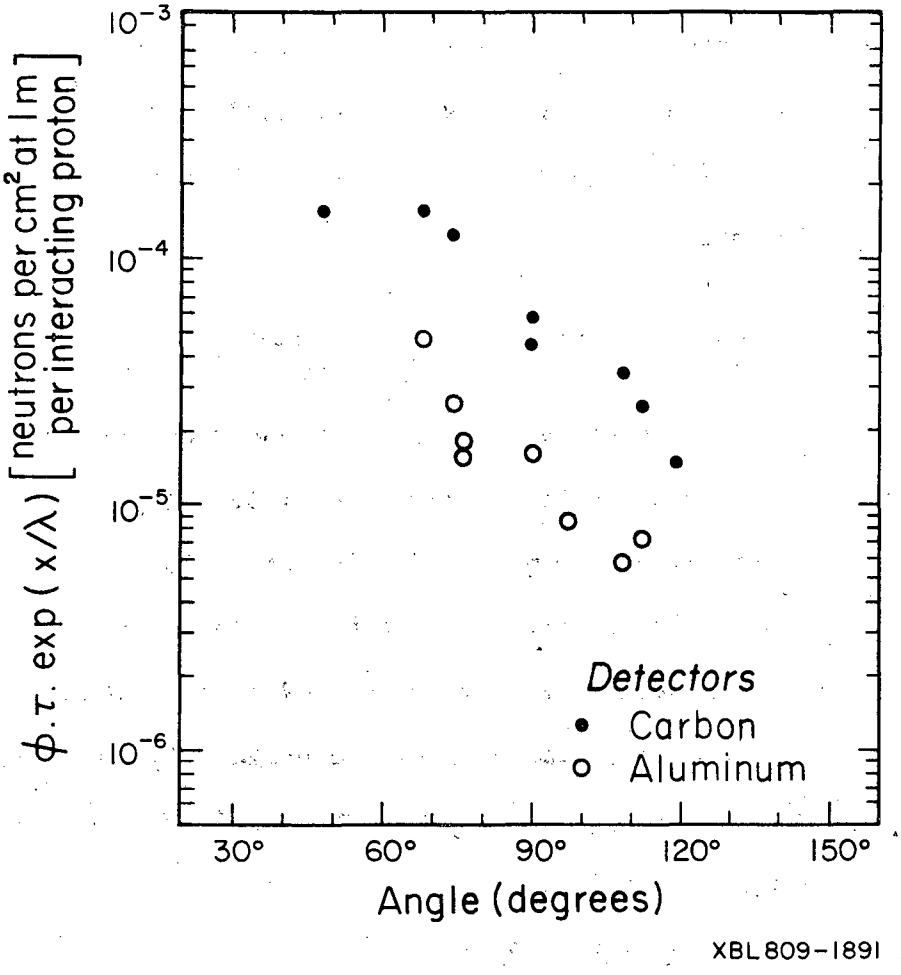

Fig. 2. Angular distribution of flux density about a thick tungsten target measured with aluminum and carbon detectors. (Rutherford Laboratory).

Table 2. Values of the Moyer Model parameters determined at the Rutherford Laboratory.

Detector	β (rad^{-1})	$H_1(E_p)$ ($Sv \cdot m^2$)
Al	2.3 ± 0.4	3.9×10^{-14}
C	2.4 ± 0.2	5.6×10^{-14}

The measurements made with three target lengths (copper target) were corrected for inverse square law and attenuation; they are shown plotted in Fig. 3. The "best fit" angular distribution parameters are given in Table 3.

(iv) Operational Measurements in CERN - West Hall

Marchall et al. (Ma 79) have reported a detailed set of measurements around the extracted beam blockhouse with a 23 GeV proton beam incident upon a 5 cm long aluminum target. Three locations are suitable for a determination of the Moyer parameter, H_1, (clean geometry free from scattered radiation from holes in the shield). The measured values at angles other than 90^o were corrected using an angular relaxation parameter of 2.3 (see previous sections).

The mean value of three determinations gave:

$$H_1(E_p) = 9.4 \times 10^{-14} \ Sv \cdot m^2 \ .$$

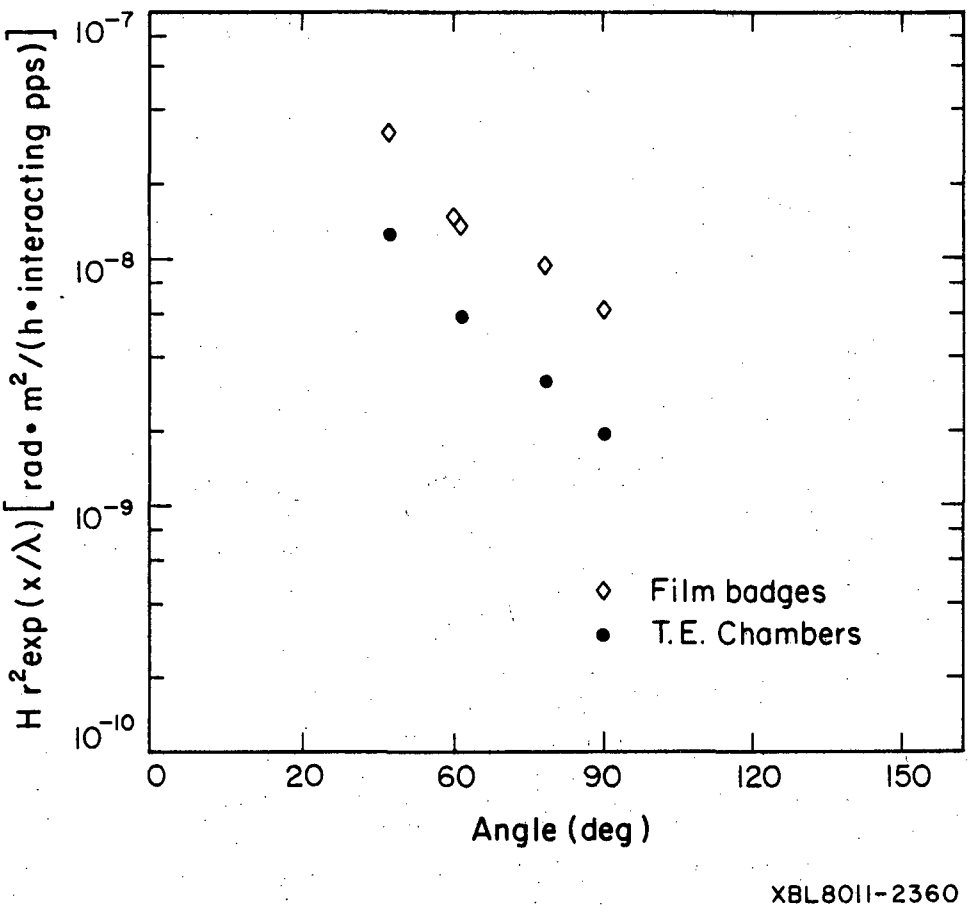

Fig. 3. Angular distribution and observed dose rate measured about a thick upper target (Argonne National Laboratory). Relative film badge measurements are also shown.

Table 3. Values of the Moyer Model parameters determined at Argonne National Laboratory.

Detector	β (rad^{-1})	Absorbed dose rate at 1 meter from the target and at 90° ($rad \cdot m^2$ per interacting proton per sec)	$H_1(E_p)$ ($Sv \cdot m^2$)
Film	2.0 ± 0.3		
Tissue Equivalent Ionization Chamber	2.5 ± 0.2	$(1.9 \pm 0.2) \times 10^{-9}$	$(2.6 \pm 0.3) 10^{-14}$

(v) Target Experiment in CERN - East Hall

Measurements on the top of and alongside a shield around a target in the CERN East Experimental Area were made during a target feasibility study at 21 GeV (Hö 79). The mean value determined for the parameter $H_1(E_p)$ was:

$$H_1(E_p) = 4.4 \times 10^{-14} \ Sv \cdot m^2 \ .$$

(vi) Experience at Brookhaven National Laboratory

Awschalom (Aw 70) has cited a determination of the Moyer Model parameter H_1 as 7.4×10^4 $(rem/h)ft^2/kw$. Assuming that this measurement was made at 30 GeV we obtain, upon conversion of units:

$$H_1(E_p) = 9.2 \times 10^{-14} \ Sv \cdot m^2 \ .$$

SUMMARY

We are interested in the values and variation with proton energy of three basic parameters so that the Moyer Model may be used to calculate shielding. These parameters are the attenuation length, λ, the angular distribution parameter, β, and the normalization constant, $H_o(E)$.

As we have seen in the previous sections there is a great deal of experimental evidence to show that β and λ are essentially independent of energy in the range of interest.

The value of attenuation length in earth was well determined in the experiments of Gilbert et al. (Gi 68) as $(1170 \pm 20)\text{kg}\cdot\text{m}^{-2}$. The experiments of Gilbert et al. (Gi 68) and Stevenson et al. (Sh 69, St 69) are consistent with a value of 1470 $\text{kg}\cdot\text{m}^{-2}$ for the attenuation length in iron and this value is consistent with the value extrapolated for iron from the value measured in earth by Gilbert et al. These values of attenuation length may be regarded as independent of proton energy for use in the Moyer Model.

As we have suggested the value of angular relaxation parameter, β, is also independent of proton energy. Table 4 summarizes the values of β determined in the shielding experiments described in the previous sections. The mean value of β obtained from these measurements is 2.3 ± 0.1.

Table 4. Summary of measured values of angular relaxation parameter, β.

Laboratory	Incident proton energy (GeV)	β (rad^{-1})
CERN - LBL - Rutherford Laboratory Collaboration	13.7	
	13.7	
	25.5	2.1 - 2.4[a,b]
Rutherford Laboratory	7.4	2.3 ± 0.4[a]
	7.4	2.4 ± 0.2[b]
Argonne National Laboratory	10.0	2.0 ± 0.3[c]
	10.0	2.5 ± 0.2[d]

Detector (a) Aluminum Activation

(b) Carbon Activation

(c) Film

(d) Tissue Equivalent Ionization Chamber

It is interesting to compare the values of β, given in Table 4 with those determined from distributions measured close to the target without any shielding present. Such distributions are presented and other results summarized by Levine et al., 1972 (Le 72). Values of β are reported as a function of threshold energy; these are shown plotted in Fig. 4. These values of β, in the angular range 60 to 120 degrees, were independent of target material (Al, Cu, W) and did not differ for proton energies of 3.7 and 23 GeV. Recent experiments at 225 GeV have confirmed this independence on proton energy (Stevenson et al., 1979) (Fa 79). The value of β corresponding to a threshold of 150 MeV taken from Fig. 4 is 2.3 ± 0.3 in agreement with the values of β determined in the experiments of the previous sections.

Because the measurements reported here are made at angles to the target in the range $60^{o} \leqslant \theta \leqslant 120^{o}$ the Moyer Model constant, H, most naturally determined is H_1 (corresponding to measurement exactly at 90^{o} to the target). The procedure adopted here has been to calculate the mean value of H_1 determined by the various experiments reported here and then to derive the best value of H_o from the relationship:

$$H_1 = H_o \, e^{-\beta\pi/2}$$

by substituting the best experimental value of β.

This procedure reduces scatter in the individual determinations of H_o due to variations in the individual values of β deduced from the separate experiments.

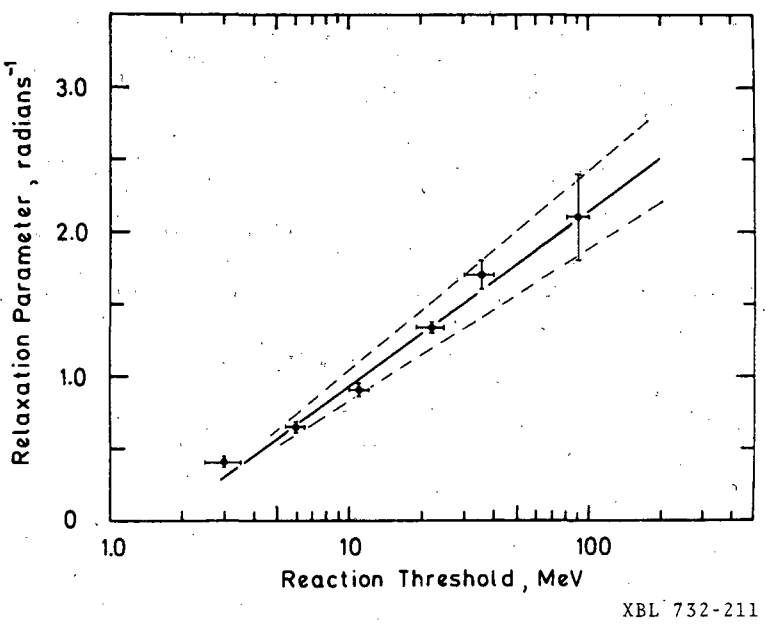

Fig. 4. Angular distribution parameter, β, as a function of detector energy threshold (after Levine et al.)

Figure 5 shows the values of H_1 determined from the measurements summarized in this paper plotted as a function of proton energy. In this figure the data for all target materials are included since Levine et al. (Le 72) showed that the flux of hadrons with energies greater than 40 MeV, at 90° to the target, is essentially independent of target material.

If we express the variation of $H_o(E_p)$ in the form:

$$H_o(E_p) = H_o E^n \tag{13}$$

the data of Fig. 5 suggest a value of n somewhat less than unity and closer to 0.75. However, the error on this value of n is large and the data are not inconsistent with a value of n = 1. For what follows in this paper we will make the conservative assumption that n = 1 and thus $H_o(E_p)$ is proportional to beam power interacting in the target. Thus:

$$H_o(E_p) = H_o \cdot E_p \tag{13a}$$

Inspection of Table 5 shows that the values obtained are in agreement within a factor of two. Variations in the value of H_o determined magnitude are to be expected because of the different shield compositions, geometries and particle detectors used.

The mean value of the values of H_o is:

$$H_o = (1.03 \pm 0.13) \times 10^{-3} \text{ Sv m}^2 \text{ J}^{-1} \quad .$$

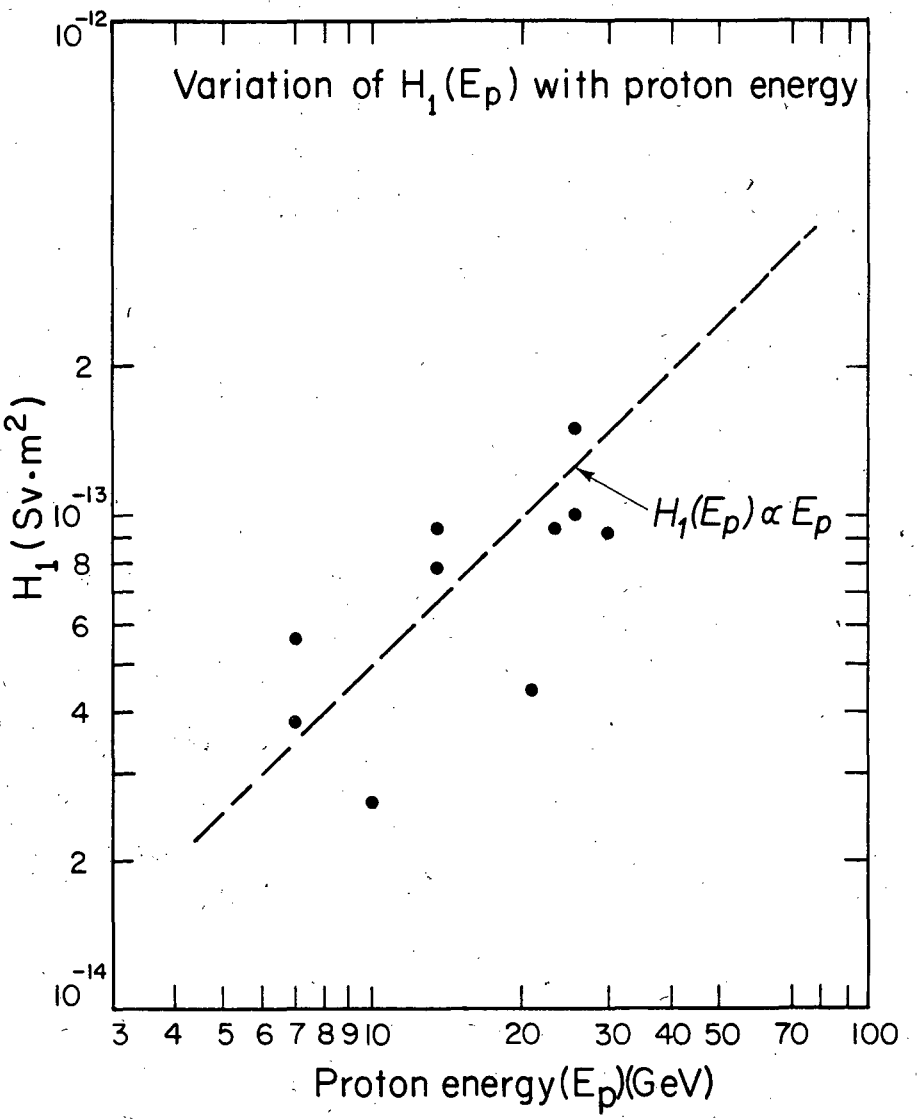

Fig. 5. Variation of H_1(Ep) with primary proton energy.

Table 5. Summary of experimentally determined values of $H_o(E_p)$.

Laboratory	Primary Proton Energy (GeV)	$H_o(E)$ ($Sv\ m^2$)		H_o ($Sv\ m^2\ J^{-1}$)
CERN, LBL, Rutherford Laboratory Collaboration	13.7	2.5×10^{-12}	(a)	1.2×10^{-3}
	13.7	3.1×10^{-12}	(b)	1.4×10^{-3}
	25.5	3.3×10^{-12}	(a)	0.81×10^{-3}
	25.5	5.0×10^{-12}	(b)	1.2×10^{-3}
Rutherford Laboratory	7.4	1.4×10^{-12}	(a)	1.2×10^{-3}
	7.4	2.1×10^{-12}	(b)	1.8×10^{-3}
Argonne National Laboratory	10.0	9.6×10^{-13}	(c)	0.60×10^{-3}
CERN				
(West Hall)	23.0	3.5×10^{-12}	(d)	0.94×10^{-3}
(East Hall)	21.0	1.6×10^{-12}	(d)	0.48×10^{-3}
Brookhaven National Laboratory	30.0	3.4×10^{-12}		0.71×10^{-3}

Mean Value: $H_o = (1.03 \pm 0.13) \times 10^{-3}\ Sv \cdot m^2\ J^{-1}$

(a) Aluminum Detector

(b) Carbon Detector

(c) LET Spectrometer

(d) REM Meter and Carbon Detector

4. An Example: The Use of the Moyer Model to Calculate Shielding For Extended Line Sources

A particular example of the value of the Moyer Model is in the calculation of transverse shielding such as might be needed, for example, along long transported particle beams with small and rather uniform beam losses.

It is simple to show (Ro 69) that for an extended uniform line source the Moyer Model of strength L GeV m^{-1} sec^{-1} the dose equivalent rate is given by:

$$H = \frac{H_o L}{a+d} \int_0^{\pi} \exp(-\beta\theta) \exp(-\, d \operatorname{cosec} \theta/\lambda)\, d\theta \qquad (14)$$

where a and d have their usual meaning and the integral of Eq. (14) may be designated by $M(\beta, d/\lambda)$ and is known as a Moyer Integral.*

Routti and Thomas have published tabulated values of Moyer Integrals with values in the ranges $0 \leqslant \beta \leqslant 10$; $0 \leqslant d/\lambda \leqslant 40$. As we have shown in the previous sections of the paper the value of β of most interest for high energy shielding is $\beta = 2.3$. The Moyer Integral $M(2.3, d/\lambda)$ is given in Table 6.

---

*Moyer Integrals are a generalized form of the Sievert Integral but account for anisotropic emission of the line source elements. The Sievert Integral is the Moyer Integral of order zero (β=0).

$$M(\beta, d/\lambda) = \int^{\pi} \exp(-\beta\theta) \quad \exp \frac{-d \operatorname{cosec}\theta}{\lambda} \, d\theta$$

Table 6. Tabulated values of the Moyer Integral, M(2.3, d/λ).

d/λ	M	d/λ	M	d/λ	M	d/λ	M
0.10	0.26570E+00	5.10	0.23505E-03	10.10	0.10211E-05	15.10	0.53891E-08
0.20	0.19609E+00	5.20	0.20997E-03	10.20	0.91833E-06	15.20	0.48751E-08
0.30	0.15221E+00	5.30	0.18762E-03	10.30	0.82593E-06	15.30	0.43779E-08
0.40	0.12158E+00	5.40	0.16768E-03	10.40	0.74287E-06	15.40	0.39460E-08
0.50	0.98960E-01	5.50	0.14991E-03	10.50	0.66821E-06	15.50	0.35568E-08
0.60	0.81623E-01	5.60	0.13404E-03	10.60	0.60109E-06	15.60	0.32061E-08
0.70	0.68008E-01	5.70	0.11989E-03	10.70	0.54075E-06	15.70	0.28900E-08
0.80	0.57123E-01	5.80	0.10725E-03	10.80	0.48649E-06	15.80	0.26052E-08
0.90	0.48301E-01	5.90	0.95964E-04	10.90	0.43770E-06	15.90	0.23485E-08
1.00	0.41070E-01	6.00	0.85883E-04	11.00	0.39383E-06	16.00	0.21172E-08
1.10	0.35089E-01	6.10	0.76876E-04	11.10	0.35437E-06	16.10	0.19087E-08
1.20	0.30101E-01	6.20	0.68827E-04	11.20	0.31889E-06	16.20	0.17207E-08
1.30	0.25915E-01	6.30	0.61632E-04	11.30	0.28697E-06	16.30	0.15514E-08
1.40	0.22380E-01	6.40	0.55199E-04	11.40	0.25826E-06	16.40	0.13986E-08
1.50	0.19381E-01	6.50	0.49446E-04	11.50	0.23244E-06	16.50	0.12610E-08
1.60	0.16825E-01	6.60	0.44300E-04	11.60	0.20921E-06	16.60	0.11370E-08
1.70	0.14638E-01	6.70	0.39696E-04	11.70	0.18831E-06	16.70	0.10251E-08
1.80	0.12761E-01	6.80	0.35576E-04	11.80	0.16951E-06	16.80	0.92435E-09
1.90	0.11145E-01	6.90	0.31888E-04	11.90	0.15259E-06	16.90	0.83347E-09
2.00	0.97496E-02	7.00	0.28587E-04	12.00	0.13736E-06	17.00	0.75154E-09
2.10	0.85418E-02	7.10	0.25632E-04	12.10	0.12367E-06	17.10	0.67769E-09
2.20	0.74941E-02	7.20	0.22985E-04	12.20	0.11134E-06	17.20	0.61110E-09
2.30	0.65834E-02	7.30	0.20614E-04	12.30	0.10024E-06	17.30	0.55108E-09
2.40	0.57902E-02	7.40	0.18490E-04	12.40	0.90260E-07	17.40	0.49695E-09
2.50	0.50982E-02	7.50	0.16588E-04	12.50	0.81274E-07	17.50	0.44815E-09
2.60	0.44936E-02	7.60	0.14882E-04	12.60	0.73185E-07	17.60	0.40416E-09
2.70	0.39644E-02	7.70	0.13354E-04	12.70	0.65904E-07	17.70	0.36449E-09
2.80	0.35007E-02	7.80	0.11984E-04	12.80	0.59350E-07	17.80	0.32872E-09
2.90	0.30939E-02	7.90	0.10756E-04	12.90	0.53450E-07	17.90	0.29647E-09
3.00	0.27365E-02	8.00	0.96548E-05	13.00	0.48139E-07	18.00	0.26738E-09
3.10	0.24221E-02	8.10	0.86673E-05	13.10	0.43357E-07	18.10	0.24116E-09
3.20	0.21454E-02	8.20	0.77817E-05	13.20	0.39051E-07	18.20	0.21751E-09
3.30	0.19015E-02	8.30	0.69872E-07	13.30	0.35175E-07	18.30	0.19618E-09
3.40	0.16864E-02	8.40	0.62745E-05	13.40	0.31684E-07	18.40	0.17695E-09
3.50	0.14965E-02	8.50	0.56350E-05	13.50	0.28541E-07	18.50	0.15961E-09
3.60	0.13288E-02	8.60	0.50613E-05	13.60	0.25710E-07	18.60	0.14397E-09
3.70	0.11804E-02	8.70	0.45463E-05	13.70	0.23162E-07	18.70	0.12986E-09
3.80	0.10492E-02	8.80	0.40841E-05	13.80	0.20866E-07	18.80	0.11714E-09
3.90	0.93297E-03	8.90	0.36693E-05	13.90	0.18799E-07	18.90	0.10567E-09
4.00	0.83000E-03	9.00	0.32968E-05	14.00	0.16937E-07	19.00	0.95317E-10
4.10	0.73872E-03	9.10	0.29625E-05	14.10	0.15260E-07	19.10	0.85984E-10
4.20	0.65775E-03	9.20	0.26622E-05	14.20	0.13750E-07	19.20	0.77567E-10
4.30	0.58588E-03	9.30	0.23926E-05	14.30	0.12389E-07	19.30	0.69975E-10
4.40	0.52206E-03	9.40	0.21505E-05	14.40	0.11164E-07	19.40	0.63126E-10
4.50	0.46536E-03	9.50	0.19330E-05	14.50	0.10060E-07	19.50	0.56949E-10
4.60	0.41497E-03	9.60	0.17376E-05	14.60	0.90650E-08	19.60	0.51378E-10
4.70	0.37015E-03	9.70	0.15621E-05	14.70	0.81690E-08	19.70	0.46352E-10
4.80	0.33028E-03	9.80	0.14045E-05	14.80	0.73619E-08	19.80	0.41818E-10
4.90	0.29479E-03	9.90	0.12628E-05	14.90	0.66346E-08	19.90	0.37729E-10
5.00	0.26319E-03	10.00	0.11355E-05	15.00	0.59794E-08	20.00	0.34039E-10

Writing (a + d) as r, the shortest distance for the line source to the outer shield surface, and expressing L as E(dJ/dZ), where E is the primary beam energy and dJ/dZ is the number of protons lost per unit length, Eq. (14) becomes:

$$H(d/\lambda,r) = \frac{H_o}{r} E(dJ/dZ)\, M(2.3,d/\lambda) \quad . \tag{15}$$

In their original paper Routti and Thomas derived a value of the normalizing constant, H_o, of 1.0×10^{-3} rem h^{-1} m GeV^{-1}·cm.s. This value was derived from data reported by Gilbert et al. (Gi 68) so as to be consistent with predictions for the shield thickness required for a 200 GeV proton synchrotron then being designed at the Lawrence Berkeley Laboratory (LB 65). The use of this value for the normalizing constant has led to some confusion which we will attempt to clarify here.

The value for the original normalizing constant is only compatible with the value $\beta = 4.0$ rad^{-1} taken by Routti and Thomas for the angular relaxation coefficient. (The value $\beta = 4.0$ rad^{-1} appeared to be the best choice at the time of publication). Subsequently, as we have seen, it was shown experimentally that β had the value 2.3 (Le 72). Rindi and Thomas (Ri 73) renormalized the data used by Routti and Thomas for this better value of β and obtained a value of 1.1×10^{-4} rem h^{-1}·m GeV^{-1}·cm.s. With a change in units this corresponds to the value:

$$H_o = 1.1 \times 10^{-6} \text{ rem}\cdot\text{m}^2\ \text{h}^{-1}\ \text{GeV}^{-1}\ \text{s}$$
$$= 3.05 \times 10^{-10} \text{ rem}\cdot\text{m}^2\ \text{GeV}^{-1}$$
$$= 1.91 \text{ rem}\cdot\text{m}^2\ \text{J}^{-1}$$
$$= 1.91 \times 10^{-2} \text{ Sv}\cdot\text{m}^2\ \text{J}^{-1} \quad .$$

This value of H_o is about a factor of 20 higher than that indicated by the data of Table 5.

The reason for the choice of the large value of H_o by Routti and Thomas was essentially to obtain agreement with shield thickness calculations by Gilbert et al. (Gi 68). These calculations were made assuming that the magnet iron in the experiments of Gilbert et al. was distributed continuously around the accelerator rather than in magnets 5 meters in length reported by open regions of approximately 2 meters. The assumption that iron was present in the magnet gaps will result in too large a value for H_o. When the presence of magnet gaps is properly allowed for, the value of H_o is reduced by a factor of 4.5. In addition, Routti and Thomas assumed that the attenuation length in iron was identical to that in earth (1170 $\text{kg}\cdot\text{m}^{-2}$). Using the proper value of 1470 $\text{kg}\cdot\text{m}^{-2}$ it may be shown that their value of H_o should be reduced by a factor of 2.6. Thus, in all, the total correction is to reduce the value quoted by a factor of 11.7 giving a value of:

$$H_o = 1.62 \times 10^{-3} \text{ Sv}\cdot\text{m}^2\ \text{J}^{-1}$$

which is in reasonable agreement with the values given in Table 5.

In the previous sections we have shown that the best value of H_o, obtained from several experiments, is 1.0×10^{-3} Sv m^2 J^{-1} and this is the value we will use in what follows.

Equation (15) may therefore be written as

$$H(d/\lambda,r) = \frac{1.0 \times 10^{-3}}{r} \cdot E(dJ/dZ)\, M(2.3,\ d/\lambda) \qquad (15a)$$

where H is in Sv s^{-1}

E is in Joules

(dJ/dZ) is in protons $m^{-1} \cdot s^{-1}$

r is in meters.

Equation (15a) may also be written as:

$$H(d/\lambda,r) = \frac{6.0 \times 10^{-8}}{r}\ E\left(\frac{dJ}{dZ}\right)\ M(2.3,d/\lambda) \qquad (15b)$$

where H is in rem h^{-1} and E is in Gev.

As we have suggested, the use of Eqs. (15a) or (15b) should predict values of dose equivalent rate to within a factor of about two.

One useful check on the claim is to compare the shield thicknesses calculated by other means. One such comparison may be made with the work of O'Brien (O'B 68) who has solved the Boltzmann transport equation in an earth/concrete shield using a spherical harmonics approximation.

O'Brien expresses his results in the form:

$$H(d/\lambda,r) = \frac{k}{r}\, E(dJ/dZ)\, B(d/\lambda) \qquad (16)$$

where k is a constant

$B(d/\lambda)$ is a barrier transmission factor

and the other symbols have their usual meaning.

The similarity between Eq. (15a) and (16) is obvious and it follows that, if these calculations are to give identical results:

$$H_o = \frac{k\ B(d/\lambda)}{M(2.3,\ d/\lambda)} \quad . \tag{17}$$

O'Brien's calculations take into account the variations in neutron spectrum produced by the water content of the shielding. Values of the barrier transmissions factors are given for concrete with various fractions of water by weight varying from 0% to 25%. O'Brien shows that as the fraction of water in the shield increases the transmission factor decreases (i.e., the shield becomes more efficient) - an effect that has been observed experimentally (Gi 68). This is due to the increasing efficiency of moderation of intermediate energy neutrons by the water in the shield and the subsequent capture of the thermal neutrons in the elements of high thermal neutron absorption cross section present in the shield. Table 7 gives an indication of the magnitude of the effect by comparing the average values of transmission factor for a shielding containing w% water by weight, B(x, w%), with that for a shield contains 6% of water by weight. (6% water by weight is typical for concrete.)

Table 7. Influence of water content of concrete on neutron transmission (after O'Brien).

Water Content (Percentage by Weight, w%)	Mean Value of $\frac{B(x, w\%)}{B(x, 6\%)}$
0	2.50
2.5	1.21
6	1.00
16	0.70
25	0.54

Inspection of Table 7 shows the variation of about a factor of two in Dose Equivalent Rate are possible from those calculated for "normal" concrete.

Equation (17) may be used to estimate a value of the Moyer Parameter H_o, from the calculations of O'Brien, and Fig. 6 shows values for the family of curves H_o $(d/\lambda, w)$ plotted as a function of d/λ. Also shown is the mean of the experimental values already described in this paper. The band of uncertainty indicated represents one standard deviation.

Within the plotted range $1 \leqslant d/\lambda \leqslant 15$ and for the range of water content in normal concrete ($2.5\% \leqslant W \leqslant 25\%$) (Ja 75). The values of H_o determined from O'Brien's calculations differ by no more than a factor of two from the mean value of the experimental data considered in this paper. This is within the level of agreement of the experiments themselves and is therefore considered quite good.

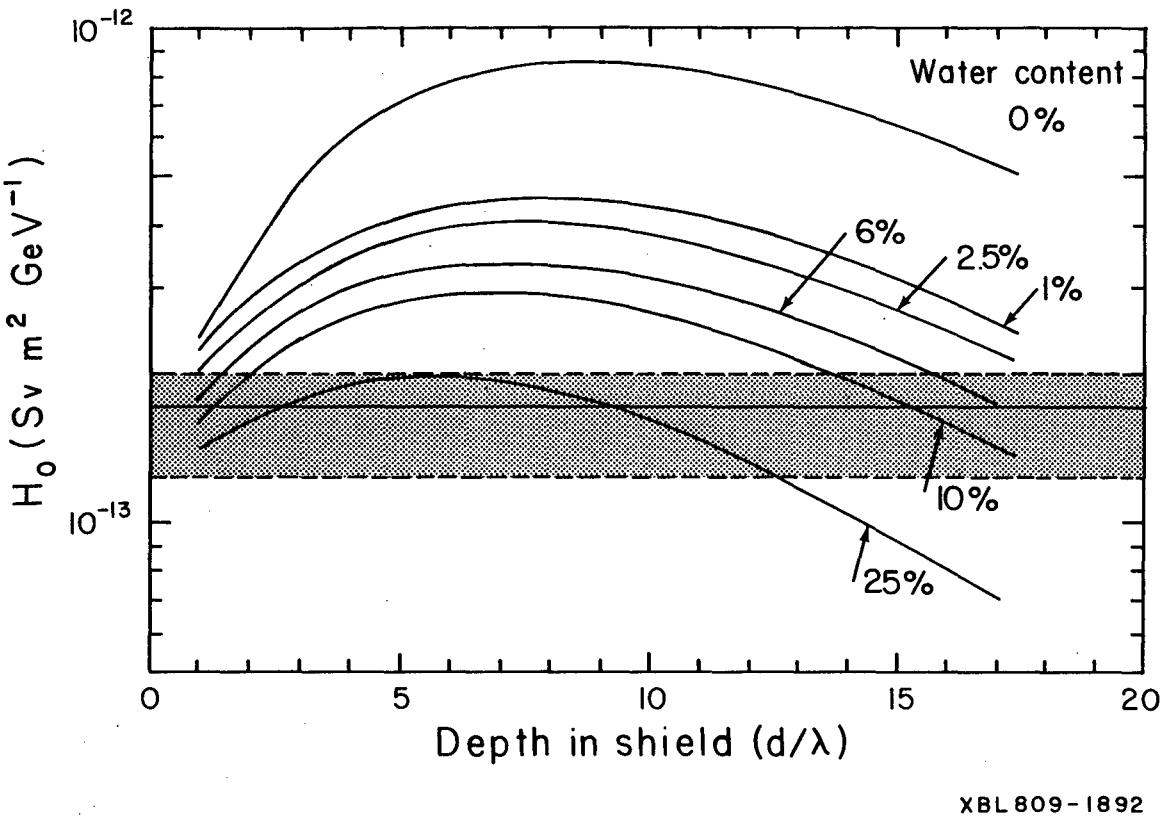

Fig. 6. Comparison of values of $H_o(d/\lambda)$ determined from the calculation of O'Brien with the experimental value. The dark band shows the region extending two standard deviations from the mean value of H_o. (95% confidence band)

5. Limitations of the Moyer Model

The Moyer Model as outlined in the previous sections may be used to calculate the intensity of the radiation field outside shielding around a target, in the energy range 1 - 50 GeV. The accuracy is probably within a factor of two, depending upon the geometry of the shielding. Two examples follow which explain the limitation in accuracy on the method, especially that of assuming a multiplicity which is independent of angle. (It should, however, be remembered that the dependence of the buildup factor on shield material has also been ignored here. We believe it to be of less importance than the effect discussed here.)

In the first case consider the situation represented in Fig. 7 where there are two cases each with the same shield thickness x and target - observer distance, r. With a small target to shield distance, secondaries with a higher average energy leaving the target at an angle, θ, other than 90 degrees can also make interactions in the shield which will contribute to the dose rate at P since the effective shield thickness x_1 is not very different from x. In case (b) however, where the target to shield distance, x_2, is very much greater than x_1, these same secondaries strike the shield at a point where they cannot contribute to the dose rate at P due to the strong exponential attenuation effect of the larger distance x^2. Thus the constant H_1 determined in the previous sections should be used in situations similar to those in which it was determined (i.e., for target shield distances ~1m).

A second circumstance is that of Fig. 8 where the observer is some distance downstream of the target and the attenuation term is so small that there can be no direct contribution by the target to the dose rate

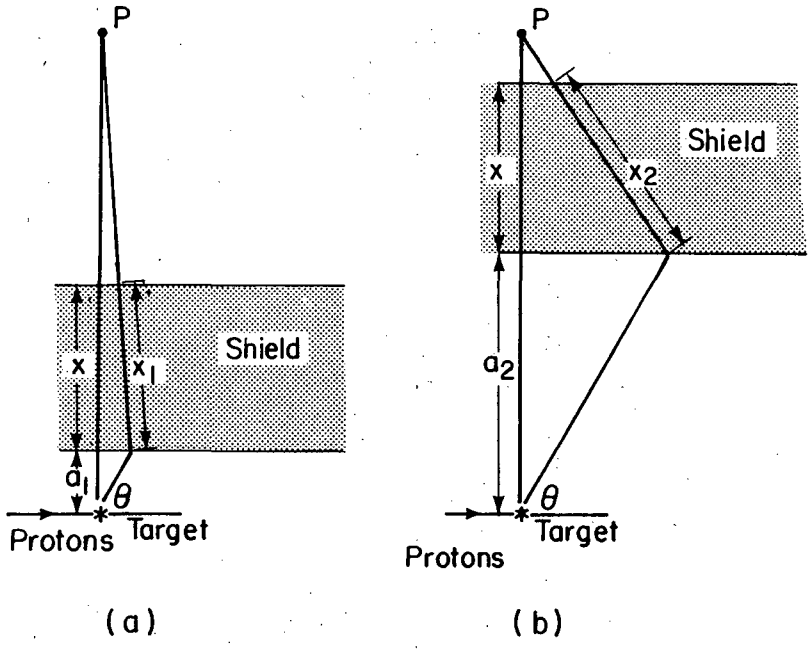

Fig. 7. Diagrams showing effect of target-shield distance on radiation intensity.

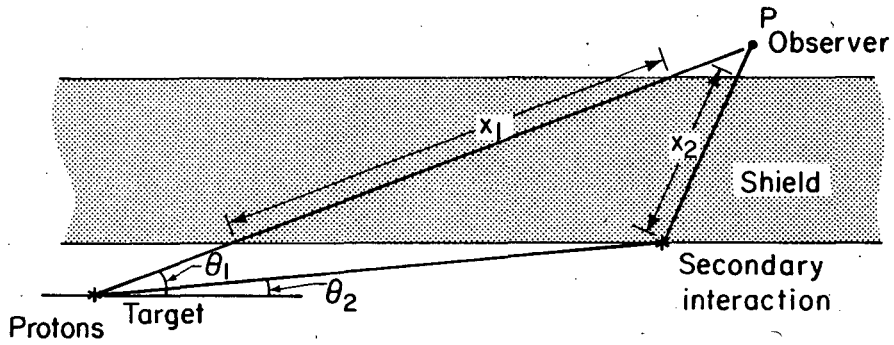

XBL 8010-2176

Fig. 8. Diagram showing effect of secondary interactions in radiation intensity.

at P. In this case only the secondary interactions in the wall of a vacuum pipe or in the inner layers of the shield, as represented in Fig. 8 can contribute to the dose rate at P. This effect is especially marked at high proton energies as can be seen from Fig. 9 where the hadron star density in the walls of a vacuum pipe of radium 5 cm placed round the target is shown plotted as a function of distance downstream of the target for different proton energies (Fa 79). These values were calculated using the Hadron Cascade code MAGKO (Ra 73). It will be seen that at the lower proton energies the secondary interactions are strongly localized in the target region, but at several hundred GeV the distribution extends to distances ~50 m or more.

6. Conclusions

In the twenty-five years or so since the needs for the Moyer Model developed there has been a great increase in our understanding of accelerator radiation phenomena. This has occurred for two reasons - firstly because the operation of high-energy proton accelerators has led to the accumulation of a great deal of experimental information (summarized in this paper) which has eliminated the uncertainties found in the early literature and secondarily because of the development of sophisticated methods of computation of the transport of high-energy radiation through accelerator shielding (Ne 80). The question therefore arises as to whether there is a continuing need for semi-empirical models such as the Moyer Model when these more sophisticated and powerful techniques are available.

In our view there will continue to be a need for methods capable of estimating shields reliably, cheaply and quickly (albeit not with

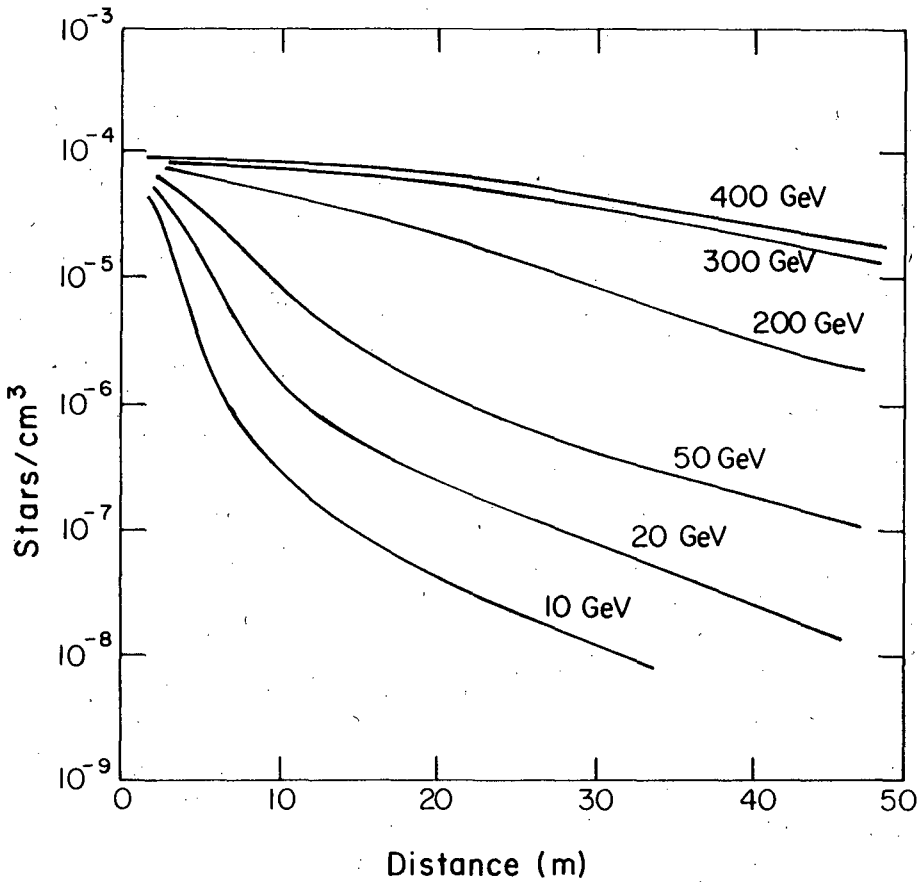

Fig. 9. Star density in a vacuum pipe around a target as a function of distance along the beam.

the precision possible with the use of a computer); such methods will facilitate rapid decisions in the preliminary stages of planning experiments or modifications to the accelerator. There will continue to be a demand, too, for methods that give sufficient physical insight into the problem of shielding to permit full utilization of the more sophisticated calculational methods.

The design of high energy accelerator shielding usually proceeds in two stages - firstly, an approximate calculation of shield thickness is made using semiphenomenological models for fairly simple geometries, and secondly, at a later stage when accelerator parameters have been more closely defined, these simple calculations are verified by the use of more sophisticated numerical methods, usually involving Monte Carlo techniques to calculate electromagnetic and hadronic cascade phenomena in the shield. These numerical techniques are not necessarily more accurate than the empirical models in estimating the intensity of radiation fields outside shielding when the geometry is simple and the primary particle energy is in a region where good experimental data are available. Under these conditions both methods can predict radiation field intensities to within a factor of two or better. The numerical techniques are of greatest value in extrapolations to new energies or for calculations with difficult geometries.

Semiphenomenological models are therefore still of great value in shielding design and have the additional advantage that they give physical insight into shielding phenomena not so evident in the more sophisticated numerical methods.

The continuing value of the Moyer Model may be seen from its use in the preliminary design for the shielding for a proton storage ring at the Stanford Linear Accelerator to operate with PEP (LB 76, Mc 73, Mc 81) and the design of shielding for the 50 GeV proton synchrotron to be built near Beijing (Ch 80).

7. Acknowledgments

The authors would like to thank their colleagues who have provided the data discussed in this paper. In particular the members of the health physics group at Argonne National Laboratory, Brookhaven National Laboratory, CERN, Lawrence Berkeley Laboratory and the Rutherford Laboratory are to be thanked for providing their experimental results and helpful discussions. We gratefully acknowledge the advice and encouragement of K. Goebel and M. Höfert of CERN, J. B. McCaslin and W. D. Hartsough of LBL during the preparation of this paper.

This work was supported by the European Centre for Nuclear Research Geneva; by the Institute of High-Energy Physics, Academia Sinica, Beijing and by the U.S. Department of Energy under Contract No. W-7405-ENG-48 with the University of California.

APPENDIX:

NOTE CONCERNING UNITS

We have tried to use coherent SI units wherever possible in this paper.

Because the use of SI units in health physics, particularly in both China and the United States, is quite new there has not been sufficient time for experience to determine the particular sub-units of the SI system which are not converted.

It has been usual to express dose equivalent rates with time expressed in hours (millirem h^{-1}, rem h^{-1}, etc.). We have chosen to utilize the unit Sv s^{-1} - principally because the second is a coherent unit of the SI system. We do not presume to infer that this is the SI unit that experience will show to be the most widely adopted.

For similar reasons in selecting units for the Moyer Model parameter, H_o, we have chosen to express it in Sv m^2 J^{-1} even though Sv m^2 GeV^{-1} is allowed (and perhaps may be more "natural" in the example cited).

For the benefit of those not entirely familiar with the International System a conversion table is given (Table A-1).

Table A-1. Conversion factors used in this report.

Quantity	Unit	
	Cgs System	SI System
Attenuation Length	1 $g \cdot cm^{-2}$	10 $kg\ m^{-2}$
Density	1 $g \cdot cm^{-3}$	10^3 $kg \cdot m^{-3}$
Dose Equivalent Rate	1 millirem h^{-1}	2.778×10^{-9} $Sv \cdot s^{-1}$
Flux Density	1 $cm^{-2}\ s^{-1}$	10^4 $m^{-2}\ s^{-1}$
Moyer Model Constant, H_o	1 rem $h^{-1} \cdot m^2$ s	2.778×10^{-6} Sv m^2
Energy	1 GeV	1.602×10^{-10} J

REFERENCES

Aw 70 Awschalom, M. (1970), "Lateral shielding for the 8 GeV and 200 GeV synchrotrons," Fermi National Accelerator Internal Report, FNAL TM-241.

Ch 80 Chu Yu-Cheng, "The Estimation of Transverse Shielding for the BPS," CERN internal technical memorandum HS-RP/TM/80-14, March 21, 1980.

De 62 De Staebler, H. (1962), "Transverse Radiation Shielding for the Stanford Two-Mile Accelerator." USAEC Report SLAC-9.

Fa 79 Fasso, A., and Stevenson, G. R. (1979), "Problemes particuliers de radioprotection poses par le fonctionnement d'un synchrotron a protons de 400 GeV," CERN HS Division Internal Report, CERN HS-RP/79-41/CF.

Gi 68 Gilbert, W. S., et al. (1968), "1966 CERN-LRL-RHEL shielding experiment at the CERN proton synchrotron," Lawrence Berkeley Laboratory, University of California report UCRL-17941.

Gi 69 Gilbert, W. S. (1969), "Shielding measurements at the CERN 25 GeV Proton Synchrotron," in Proceedings of the Second International Conference on Accelerator Dosimetry held at Stanford Linear Accelerator Center, November 5-7, 1969, USEAC Report CONF-691101, p. 323.

Ho 66 Howe, H. J., Oldfield, G. V., Srenianski, D. J., and Wheeler, R. V. (1966), "On the shielding of the external proton tunnel area of Argonne's zero gradient synchrotron," Argonne National Laboratory Internal Report, ANL-7273.

Ho 79 Höfert, M., Chu Yu-Cheng, Hanon, J. M. and Sanchez, J. (1979), "Radiation protection measurements around the e_{18} beam in the PS Experimental Hall," CERN HS Division Internal Report, CERN HS-RP/044.

Ja 75 Jaeger, R. G. (Ed.) (1975), Engineering Compendium on Radiation Shielding Vol. 2, "Shielding Materials," Springer-Verlag (Heidelberg).

LB 65 "200 BeV Design Study" (2 Vols) (1965), Lawrence Berkeley Laboratory Internal Report, UCRL-1600.

LB 76 "PEP Conceptual Design Report" (1976), Lawrence Berkeley Laboratory Internal Report, LBL-4288.

Le 72 Levine, G. S., Squier, D. M., Stapleton, G. B., Stevenson, G. R., Goebel, K., and Ranft, J. (1972), "The angular dependence of dose and hadron yield from targets in 8 GeV/c and 24 GeV/c extracted proton beams," Particle Accelerators 3, 91-104.

Ma 79 Marchall, H. (1979), CERN private communication.

Mc 73 McCaslin, J. B. and Thomas, R. H. (1973), "Neutron Shielding for PEP," Lawrence Berkeley Laboratory Internal Document--PEP Note 76, Nov. 1, 1973.

Mc 81 McCaslin, J. B. (1981), "Moyer Model Approximations for Point and Extended Beam Losses," to be submitted to Health Physics.

Mo 61 Moyer, B. J. (1961), "Evaluation of shielding required for the improved Bevatron," Lawrence Berkeley Laboratory, University of California, Report UCRL-9769 (unpublished).

Mo 62 Moyer, B. J. (1962), "Method of calculation of the shielding enclosure for the Berkeley Bevatron," in Proceedings of the First International Conference on Shielding Around High Energy Accelerators, Presses Universitaires de France, Paris, p. 65.

Ne 80 Nelson, W. R., and Jenkins, T. M., (eds.), (1980), "Computer Techniques in Radiation Transport and Dosimetry." Plenum Press (New York).

O'B 68 O'Brien, K. (1968), "Tables for the determination of the lateral shielding requirements of high energy accelerators," U.S. Department of Energy, Environmental Measurements Laboratory, New York, Report HASL-203.

Pa 73 Patterson, H. W. and Thomas, R. H. (1973), "Accelerator Health Physics," Academic Press, New York.

Pe 66 Perry, D. R. (1966), "Neutron Dosimetry Methods and Experience on the 7 GeV Proton Synchrotron, Nimrod," Proc. Symp. on Neutron Monitoring for Radiological Protection IAEA, Vienna, p. 355.

Ra 73 Ranft, J. (1973), "Hadron cascade calculations at large angles to the interaction point," CERN Internal Report, CERN LAB II-RA/73-2.

Ri 73 Rindi, A. and Thomas, R. H. (1973), "The Radiation Environment of High-Energy Accelerators." Ann. Rev. Nucl. Sci., 23, 315.

Ro 69 Routti, J. T., and Thomas, R. H. (1969), "Moyer integrals for estimating shielding of high-energy accelerators," Nuc. Inst. and Methods, 76, 157-163.

Ro 72 Routti, J. T., and van de Voorde, E. M. (1972), "Dose estimates of the shielding of the CERN intersecting storage range by the Moyer method," Nuclear Engineering and Design, 21, 421-434.

Sh 69 Shaw, K. B. and Stevenson, G. R. (1969), "Radiation studies around extracted proton beams at Nimrod," Proc. 1969 Particle Accelerator Conference Washington, D.C., March 1969. IEEE Trans. Nucl. Sci. NS-16 No. 3, Part 1, p. 570.

Sm 65a Smith, A. R., McCaslin, J. B. and Pick, M. (1965), "Radiation field inside a thick concrete shield for 6.2 BeV incident protons," Proc. First Symposium on Accelerator Dosimetry and Experience, Brookhaven National Laboratory, November 3-5, 1965, USAEC Report CONF-651109, p. 365.

Sm 65b Smith, A. R. (1965), "Some experimental studies at the 6.2 BeV Berkeley Bevatron," in Proceedings of the First Symposium on Accelerator Radiation Dosimetry, held at Brookhaven National Laboratory, November 3-5, 1965, USAEC Report CONF-651109, p. 224.

So 57 Solon, L. R. (ed.) (1957), Conference on Shielding High-Energy Accelerators, New York, April 11-13, 1957. USAEC Report TID-7545.

St 69 Stevenson, G. R., Shaw, K. B., Hargreaves, D. M., Lister, R. P., and Moth, D. A., "Measurements of the Radiation Field Around the X2 Extracted Proton Beam," Rutherford Laboratory Report RHEL/M 148, Jan. 1969.

We 63 Wenzel, W. A. (1963), "Bevatron external proton beam," Proc. Int. Conf. on High-Energy Accelerators, Dubna. August 21-27 1963, p. 698. Atomizdat Moscow, 1964.

This report was done with support from the Department of Energy. Any conclusions or opinions expressed in this report represent solely those of the author(s) and not necessarily those of The Regents of the University of California, the Lawrence Berkeley Laboratory or the Department of Energy.

Reference to a company or product name does not imply approval or recommendation of the product by the University of California or the U.S. Department of Energy to the exclusion of others that may be suitable.

TECHNICAL INFORMATION DEPARTMENT
LAWRENCE BERKELEY LABORATORY
UNIVERSITY OF CALIFORNIA
BERKELEY, CALIFORNIA 94720